Atmospheric Research 160 (2015) 15–27

Contents lists available at ScienceDirect

Atmospheric Research

journal homepage: www.elsevier.com/locate/atmos

Assessment of different raindrop size measuring techniques: Inter-comparison of Doppler radar, impact and optical disdrometer

Thumree Sarkar, Saurabh Das, Animesh Maitra *

Institute of Radio Physics and Electronics, University of Calcutta, 92, A. P. C. Road, Kolkata 700009, India

ARTICLE INFO

Article history:
Received 3 November 2014
Received in revised form 23 February 2015
Accepted 1 March 2015
Available online 8 March 2015

Keywords:
Drop size distribution
Joss–Waldvogel disdrometer
Micro rain radar
Laser precipitation monitor
Z–R relation

ABSTRACT

The performances of three instruments namely, Joss–Waldvogel disdrometer, laser precipitation monitor and micro rain radar, are assessed in terms of their ability to measure rain related parameters and to better understand the dependency of measured parameters on the working principles of the instruments. Twenty one rain events of year 2013 pertaining to South-West monsoon are considered for this study. The raindrop size distributions measured by the three instruments show good agreement only for medium sized (1–3 mm) raindrops and for medium rain rates (up to 30 mm/h). However, the mutual agreements are not very good in case of large (>5 mm) and very small raindrops (<0.5 mm) as well as for very high rain rates (>30 mm/h) and very high radar reflectivity factor (>40 dB). The radar reflectivity–rain rate relation is also studied using linear regression method which shows distinct differences for these instruments, indicating the high sensitivity of Z–R relation on the instrumental measuring principle.

1. Introduction

Information on spatio-temporal variability of rainfall characteristics is important in view of the increasing number of extreme rain events worldwide. Rain in one hand can be of major importance for socio-economic development of a country. On the other hand extreme rain events can be very hazardous, can cause severe economic loss, and can even endanger human safety. Studies of spatial and temporal variability of rain also contribute towards microphysical understanding of precipitation (Ulbrich and Atlas, 2007; Thurai et al., 2012, 2014). Further, the remote sensing of rain using radars is based on the association between ground rain rate (R) and radar reflectivity factor (Z), which varies widely for different regions as well as for different rain types (Campos and Zawadzki, 2000). Even after numerous numbers of studies, the variability in the Z–R relation as well of drop size distributions (DSDs) is a topic of extreme importance. This is especially true in the case of a tropical region, where the weather conditions are markedly different from that of temperate regions.

There is a dearth of comprehensive ground based observations of tropical rain features. The effective study of spatio-temporal variations of rain requires an intense network of instruments working concurrently. However, the instruments used for this kind of study must be economical and robust to endure weather variability during different seasons (Frasson et al., 2011).

The variability in DSDs comes mainly from instrumental and physical variability like distance and time difference between the instruments. If the observations are taken at a single location and simultaneously by various instruments, the physical variability will be negligible. Thus the variability in the measurements will occur due to the instruments working on different principles and sampling uncertainty.

* Corresponding author at: Institute of Radio Physics and Electronics, University of Calcutta, 92, Acharya Prafulla Chandra Road, Kolkata 700009, India. Tel.: +91 33 2350 9116x28 (office); fax: +91 33 2351 5828.
E-mail addresses: thumrees1988@gmail.com (T. Sarkar), das.saurabh01@gmail.com (S. Das), animesh.maitra@gmail.com, am.rpe@caluniv.ac.in (A. Maitra).

http://dx.doi.org/10.1016/j.atmosres.2015.03.001
0169-8095/

Although several studies of instrumental inter-comparison have been reported using various types of disdrometers and radars in the temperate region (Campos and Zawadzki, 2000; Tokay et al., 2001; Frasson et al., 2011), such studies are sparse in the tropical region. Tropical DSDs of some extreme weather conditions like freezing rain and snow storm have been studied by various researchers (Chen et al., 2011; Zhou et al., 2009; Sun and Zhao, 2010) using varied instruments ranging from impact disdrometer, Doppler radar wind profiler, optical disdrometer, etc. The seasonal variations of rain DSDs for various locations have also been studied by researchers (Tokay et al., 1998; Reddy and Kozu, 2003; Rao et al., 2009). However, no effort has yet been made to quantify the instrumental limitations with respect to the variation of raining conditions at tropical locations where rather an extensive study is required.

The aim of the present study is to compare the performance of three instruments: (i) impact type Joss Waldvogel disdrometer (JWD, Disdromet RD-80), (ii) laser precipitation monitor (Theis Clima LPM) and (iii) frequency modulated continuous wave (FMCW) Doppler radar (Metek MRR-2). The instruments operate on different working principles, so an inter-comparison among these instruments can help to understand the instrumental bias in DSD estimation and consequent implications in the Z–R relation. This will also be helpful to identify the valid rain rate ranges of the different instruments for radar reflectivity estimation from DSDs, which is a key factor of radar remote sensing.

The present study considers 21 rain events with total duration of 1549 min of Indian summer monsoon during June–August 2013. The rain DSDs, rain rate and radar reflectivity factors are studied with the help of the above mentioned instruments deployed at the Institute of Radio Physics and Electronics, University of Calcutta, Kolkata (22°34′N, 88°29′E), India. The instruments are operated at the same location within a distance of 3 m and the recording times of the instruments are accurately calibrated to minimize the spatial and temporal variability of rain. Thus uncertainties in measurement of instruments can come from mainly two causes, 1) Instrumental working principle and 2) Sampling uncertainties (Jaffrain and Berne, 2011). However in the present study it is not possible to measure the sampling uncertainty in the absence of a network of instruments working with the same principle. Again as the distances between the instruments are very small to create a significant spatial variability, the sampling induced error will be much less. The error reported here is a summation of both sampling error as well as instrumental working principle. However the results clearly state the range of each instrument to measure rain integral parameters efficiently, thus the reason of our study is well supported.

2. Instrumental details

2.1. Joss–Waldvogel disdrometer

The impact type Joss–Waldvogel disdrometer (JWD, Distromet RD-80) is commonly used to measure rain DSDs. This electro-mechanical device was primarily designed for estimating the radar reflectivity factor from measured DSDs (Tokay et al., 2001). The instrument transforms the mechanical impacts of hydrometeors on its sensor to an electric pulse whose amplitude is a function of the size of the impacting drop. The sampling area of the transducer is 50 cm^2. In the processor part of the instrument, the drops are sorted in 20 size bins ranging from 0.3 to 5.5 mm. The intervals of the size bins are not uniform. The JWD measures DSDs with about $\pm 5\%$ accuracy (Tokay and Short, 1996). The specifications are also listed in Table 1.

There is a significant progress in disdrometer technology but JWD is still very dependable and a robust instrument for ground based measurements of DSDs, as the instrument can withstand weather hazards and can be operated continuously (Tokay et al., 2001). Wind and surrounding acoustic noise are two sources of errors which can be reduced by proper installation of the instrument in a noise-free environment. Again the ringing of styrofoam cone at high rain rates, known as dead time error, is another source of error which can be corrected using a correction matrix (Sheppard and Joe, 1994). However, the correction matrix has a tendency to modify DSDs. At lower rain rates the correction matrix does not implement any correction to DSDs but it increases the higher moments of DSDs such as rain rate and reflectivity (Tokay and Short, 1996; Tokay et al., 2013). On the other hand at high rain rates, it changes DSDs markedly but rain rate and reflectivity factor do not change much (Caracciolo et al., 2006). Thus we used the raw data without applying the correction matrix in our study.

The DSD (mm^{-1} m^{-3}) is normalized using the following relation,

$$N(D_i) = \frac{n_i}{A.t.v(D_i).\Delta D_i} \tag{1}$$

where, $N(D_i)$ is the normalized drop concentration which can be defined as the number density of drops corresponding to size class i per unit volume. n_i is the measured number of drops in size class i, D_i is the drop diameter of class i, A is the cross sectional area (50 cm^2 for JWD) of sensor, t is the temporal resolution (30 s), $v(D_i)$ is the terminal drop velocity of class i and ΔD_i is the diameter difference between two consecutive classes. The rain rate and radar reflectivity factor are also calculated using the generalized equations:

$$R = \frac{\Pi}{6}.\int_0^\infty D^3.v(D).N(D)dD \tag{2}$$

$$Z = \int_0^\infty N(D).D^6 dD. \tag{3}$$

2.2. Laser precipitation monitor

Laser precipitation monitor (LPM) is an optical disdrometer which measures precipitation drop size and drop velocity at ground level simultaneously. LPM uses a 780 nm infrared

Table 1
Specifications of JWD.

Operating Principle	Mechanical
Surface type	Styrofoam
Sampling area	50 cm^2
Temporal resolution	30 s
Drop size range	0.31–5.5 mm
Drop size bins	20

Table 2
Specifications of LPM.

Operating principle	Optical
Sampling area	46 cm^2
Wavelength of laser signal	780 nm
Temporal resolution	60 s
Drop size range	0.125–8 mm
Drop size bins	22
Velocity range	0–10 m/s
Velocity bins	20

parallel light beam with a cross section area of approximately 46 cm^2. Every hydrometeor falling through the laser beam reduces the signal, and from the amplitude reduction measurements, the diameter of the falling particle can be measured. The fall speed of the particle is estimated from the duration of reduced signal. In the case of our study we have used one minute accumulation mode which yields a 22 × 20 matrix each minute containing a summary of all drop concentration recorded. This matrix for each minute stores information about 22 diameter classes ranging from 0.125 to 8 mm, and 20 velocity classes ranging from 0.2 m/s to 10 m/s. The DSDs and velocity class intervals are non-uniform for LPM also. The specifications of LPM are also listed in Table 2. The raw DSD data is normalized using Eq. (1). The rain rate and radar reflectivity are then calculated from DSDs using the relations (2) and (3).

This instrument is useful for all real time applications as there is no effective time delay of the output due to the optical working principle of LPM (Lanzinger et al., 2006). Moreover as it is a contactless instrument, errors introduced due to evaporation and retention are absent here. However, the instrumental readings are reported to be very much inconsistent in windy condition (Frasson et al., 2011). It is also reported that though it measures low rain rates quite efficiently, but it over-estimates high rain rates due to misinterpretation of multiple simultaneous drops as a large single drop (Lanzinger et al., 2006).

2.3. Micro rain radar

Micro rain radar (MRR) is a vertically pointing FM-CW radar that measures the evolution of DSD spectra and drop velocity of rain above ground. It is a highly reliable system which can be used in remote sensing of extreme environments as it requires minimum maintenance. It transmits 24.1 GHz frequency using 50 mW power and the temporal resolution of the instrument is 30 s. The device can detect rain DSDs from 0.25 mm to 6 mm range. The radar uses Doppler principle to measure fall velocity of hydrometeors, and using Gunn and Kinzer's (1949) relation, the DSDs are evaluated. Rain rate and radar reflectivity are calculated from measured DSDs using relations (2) and (3). MRR gives vertical profile of DSDs, rain rate and radar reflectivity up to 6 km. The total height is covered in 30 steps with 200 m resolution. To compare the ground DSDs, rain rate and radar reflectivity factor of the above mentioned three instruments, we have taken the 200 m height range DSD data of MRR, and calculated the rain rate and reflectivity of that height. The specifications of MRR are also listed in Table 3.

Table 3
Specifications of MRR.

Operating principle	Radio wave
Antenna type	Offset parabolic
Frequency of wave	24 GHz
Transmit power	50 mW
Beam width	2°
Antenna diameter	600 mm
Temporal resolution	30 S
Drop size range	0.25–5.03 mm
Drop size bins	46
Height resolution	200 m

It was reported that wind motion correction in MRR data may degrade the retrieved product (Peters et al., 2005). Thus the zero vertical wind assumption is taken in deducing DSDs from fall velocity using Gunn–Kinzer relations. Another important consideration in MRR is the attenuation of signal strength at 24 GHz due to rain and water vapor, however, it can be neglected for path lengths (200 m) considered here.

In addition, we have used this radar data to identify the rain type, namely, stratiform and convective. Radar reflectivity profile indicates the presence of melting layer by a radar bright band signature (Das et al., 2010; Peters et al., 2002; Fabry and Zawadzki, 1995). The bright band is signified by an abrupt enhancement in vertical radar reflectivity profile due to the change in dielectric properties of melting ice at that level (Gunn and Kinzer, 1949; Kain et al., 2000; Sarkar et al., 2014). It is to be noted here that, there exist various other methods to classify rain types using rain rate, radar reflectivity factor and other related parameters (Islam et al., 2012; Steiner et al., 1995). We have used the bright band signature to classify rain for its simplicity. From the presence of melting layer signature, the nature of rain, whether stratiform or convective or mixed can be determined (Fabry and Zawadzki, 1995).

3. Methodology

We have considered 21 rain events with total 1549 min data from JWD, MRR and LPM. The details of the events studied are given in Table 4. The average DSD values are compared event

Table 4
Event specifications.

Date (DD.MM.YY)	Time (IST)	Highest rain rate (mm/h)	Event type
15.06.13	10:08–10:32	50	Convective
17.06.13	10:55–11:30	42	Convective
18.06.13	12:59–14:24	75	Convective
19.06.13	9:55–11:30	7	Stratiform
27.06.13	5:37–7:22	25	Mixed
29.06.13	2:42–3:14	22	Stratiform
29.06.13	17:08–19:40	30	Mixed
06.07.13	12:05–12:26	35	Convective
13.07.13	6:02–9:41	3	Stratiform
15.07.13	12:25–12:44	15	Convective
16.07.13	13:17–13:47	60	Convective
17.07.13	12:41–12:58	50	Mixed
20.07.13	13:03–13:21	90	Convective
21.07.13	12:24–12:45	40	Mixed
22.07.13	14:13–14:34	45	Mixed
23.07.13	8:36–9:02	70	Convective
25.07.13	13:35–14:11	6	Stratiform
26.07.14	3:15–11:05	45	Mixed
27.07.13	3:19–10:37	35	Mixed
03.08.13	8:01–9:10	40	Convective
05.08.13	11:54–12:16	16	Stratiform

wise as well in different rate categories. First, three case studies are presented, representing three different rain types, namely, convective, mixed and stratiform rains. Then, the entire collection of rain events is grouped into six rain rate classes and the average DSD characteristics are studied. Rain rate and radar reflectivity characteristics are also taken into account for all the three instruments to study the performances of these instruments in a statistical basis. Furthermore, the *Z–R* relations obtained from the three instruments are compared.

4. Results and discussions

4.1. Case studies

The case studies represent three rain events, a purely convective event on 18 June 2013 with highest rain rate of 150 mm/h, a mixed event on 26 July 2013 with highest rain rate of 45 mm/h and a purely stratiform event with highest rain rate of 3 mm/h as recorded on 13 July 2013.

4.1.1. Convective event

The event occurring on 18 June 2013 was a convective event, which is confirmed from Fig. 1(d), where the MRR rain rate profile shows no signature of melting layer (Das et al., 2010; Fabry and Zawadzki, 1995). The event duration is 1.5. h. and the ground rain rate is very high (>50 mm/h) for a long time as shown in Fig. 1(a). In this severe rain rate event, LPM shows highest rain rate of 140 mm/h whereas MRR and disdrometer show much less rain rate (<100 mm/h). The radar reflectivity factors in Fig. 1(b) show a difference for different instruments, especially for the regions where rain rate is very high. The differences in rain rate and radar reflectivity factor of these instruments can be explained in terms of DSD characteristics obtained from the same instruments as shown in Fig. 1(c), in which the mean concentration values of drops per unit volume are plotted at different drop sizes. As from relations (2) and (3) we can see that rain rate and radar reflectivity factor are respectively the 3.67th moment (as the terminal fall velocity of drops is proportional to 0.67th moment of DSDs) and sixth moment of DSDs. Thus the presence of large drops increases *R* and *Z* significantly. The effect of large drop is more on *Z* since it is the sixth moment of DSDs; however the increase in rain rate is more sensitive to the median volume diameter, or shift of the mean DSDs towards large drop size. For this particular event, drop size measured by all the three instruments matches for the region 1–3 mm. For large drop sizes greater than 3 mm, LPM shows high concentration of drops than other instruments and estimates some very large

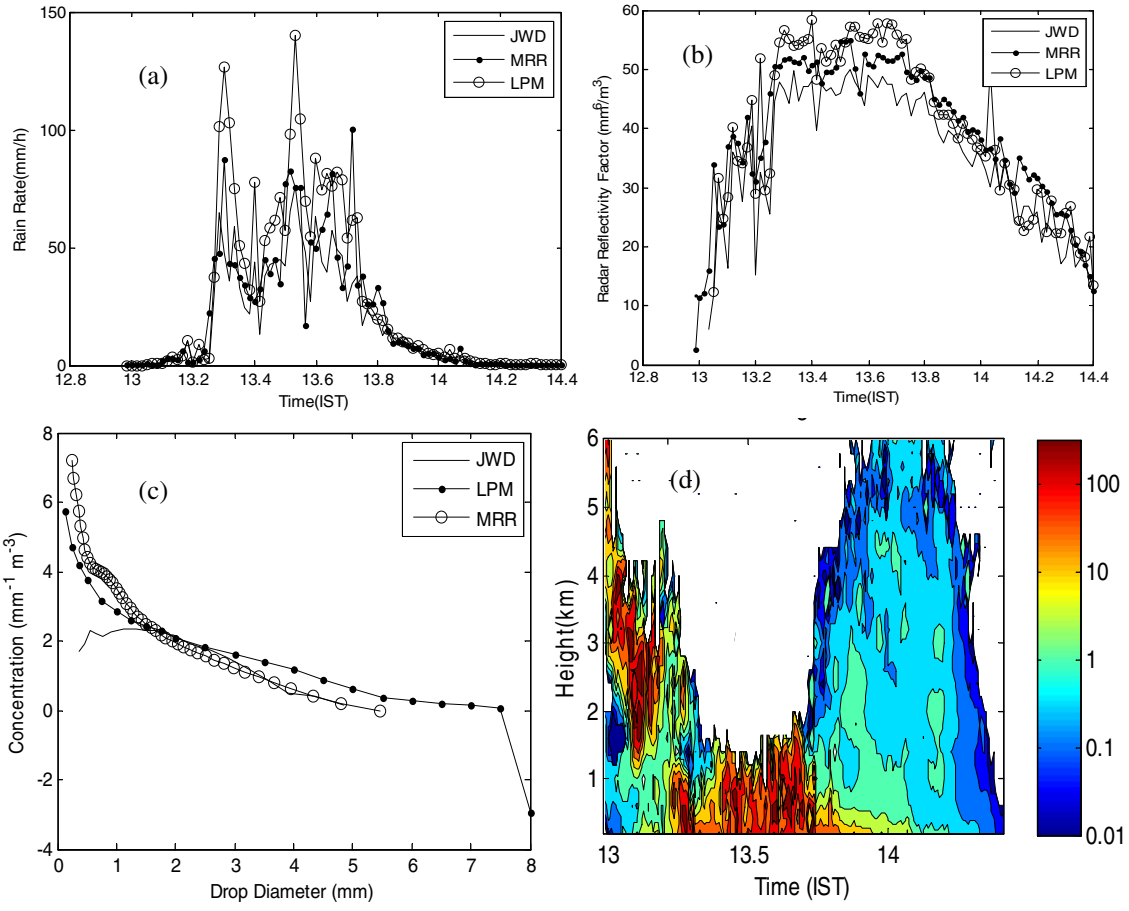

Fig. 1. High rain rate event of 18 June 2013: (a) Ground rain rate, (b) Radar reflectivity (c) Ground DSDs' concentration in log10 scale for different drop diameters and (d) Height profile of rain rate in mm/h obtained from MRR.

drops of diameter 6–7 mm which may not be realistic. The large drop size of 6–7 mm in case of LPM may trigger the value of Z to be very high. Moreover, the presence of high concentration of large drops will also shift the mean diameter towards high end resulting in high rain rates. MRR and JWD measure similar concentration of drops up to 4 mm size. For DSDs lower than 1 mm, MRR and LPM show distinctly higher concentration of raindrops than JWD, confirming the inability of impact type disdrometer to measure very small drops in high rain rate events. This is due to the fact that during high rain rates, the styrofoam cone diaphragm of JWD suffers from ringing due to the impact of large raindrops and the impact of small drops are submerged in the noise level of the instrument.

4.1.2. Mixed event

The next event, occurring on 26 July 2013, is a mixed event with duration of 8 h. Fig. 2(d) shows the rain rate height profile obtained from MRR. During 3–6 h and 8–11 h, the presence of melting layer is observed at the height of 5 km, confirming the occurrence of stratiform rain (Fabry and Zawadzki, 1995). However, during 6–8 h, the absence of melting layer confirms the presence of convection. For the convective part of the event the rain rate as shown in Fig. 2(a) reaches up to 45 mm/h and all the instruments are in quite good agreement with one another. The low rain rate stratiform part with rain rate below 10 mm/h also shows good agreement among all the instruments. However in the case of radar reflectivity factor shown in Fig. 2(b), MRR shows somewhat higher value than JWD but almost matches with LPM. The similarity in *Z* for LPM and MRR can be explained by the presence of large drops (6 mm) in both cases. However as JWD does not measure drops larger than 4 mm, the *Z* value calculated from the DSDs data of JWD is somewhat less than that of the calculated value from DSD data of MRR and LPM. As already mentioned, LPM overestimates drops larger than 4 mm compared to that observed by MRR. Fig. 2(c) shows good agreement between DSDs for all the instruments between 1 and 3 mm. For lower than 1 mm size the drop concentration in JWD is considerably less than LPM and MRR. In this case also, very small drops (<0.5 mm) in JWD is under estimated. The presence of 7 mm drop can be seen in case of LPM which should be an erroneous value for the reason already pointed out (Lanzinger et al., 2006) in Section 2.2.

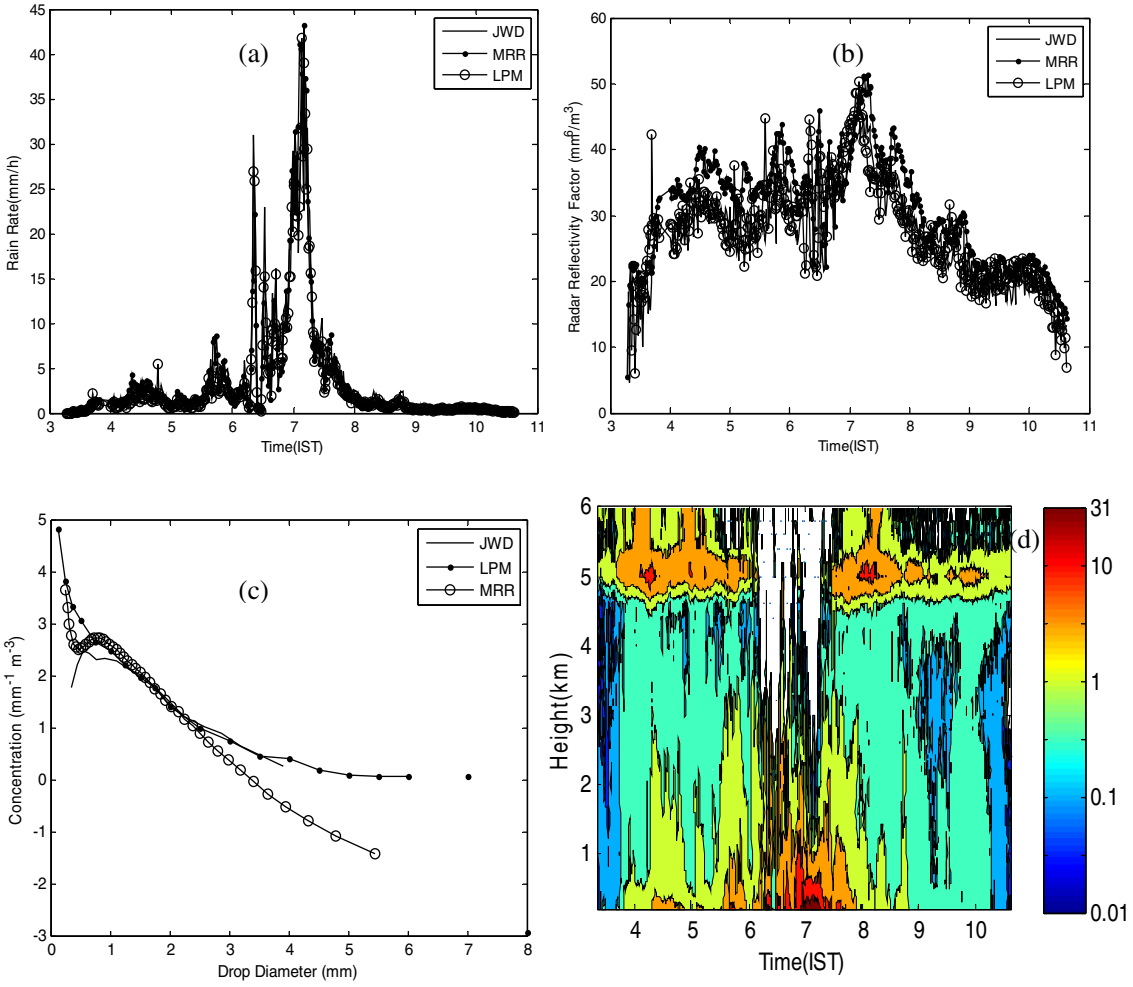

Fig. 2. Medium rain rate event of 26 July 2013: (a) Ground rain rate, (b) Radar reflectivity (c) Ground DSDs' concentration in log10 scale for different drop diameters and (d) Height profile of rain rate in mm/h obtained from MRR.

4.1.3. Stratiform event

The third event, recorded on 13 July 2013 with duration of 3.5 h, is a purely stratiform event with strong presence of melting layer at 5 km as shown in Fig. 3(d). The rain rate of the event never exceeded 4 mm/h. Here also the agreement of rain rate measurements shown in Fig. 3(a) is very good for JWD, MRR and LPM. Nevertheless, in this case also the radar reflectivity factor shows higher values for MRR than for LPM and JWD. The cause can be explained from Fig. 3(c), where MRR records large drops of 6 mm whereas LPM records drop size of 5 mm and JWD 4 mm. Due to the presence of large drops in the case of MRR the Z value is greater than that obtained from LPM and JWD. The observations of DSDs in the size range of 1–3 mm are in good agreement for all the instruments as shown in Fig. 3(c).

4.2. Statistical results

4.2.1. DSD comparison for different rain types

All the events categorized in three rain types are grouped and the statistical pictures of average DSDs' variation for the rain types are shown in Fig. 4. Fig. 4(a) shows the average DSD concentration with drop diameter in case of convective events. Fig. 4(b) summarizes the DSD variations in the three instruments for mixed rain regimes and Fig. 4(c) shows the same taking into account all stratiform rain events. The figures depict that the matching between all the three instruments is quite good in the range of 1–3 mm drop size. However for lower than 1 mm drop size LPM and MRR show significantly high concentration of drops than recorded by JWD. For drops larger than 3 mm, LPM shows the highest concentration and MRR shows the lowest concentration among all three instruments.

4.2.2. DSD comparison for different rain rates

For the purpose of studying the DSD variability by the three instruments, the total dataset has been grouped in six parts from very low rain rate regime (<1 mm/h) to very high rain rate (>20 mm/h) and average DSDs are computed for each part. The results are shown in Fig. 5.

From this statistical analysis, we can point to some important aspects of the instruments under different raining conditions. From Fig. 5, we can see that irrespective of rain rate variations, the contribution of medium sized (1–3 mm) raindrops from all the instruments is in close proximity. It is also evident from the study that, for every rain rate class JWD gives lower concentration of very small (<0.5 mm) drops compared to other instruments indicating lesser sensitivity of JWD than optical disdrometer and Doppler radar for small drop

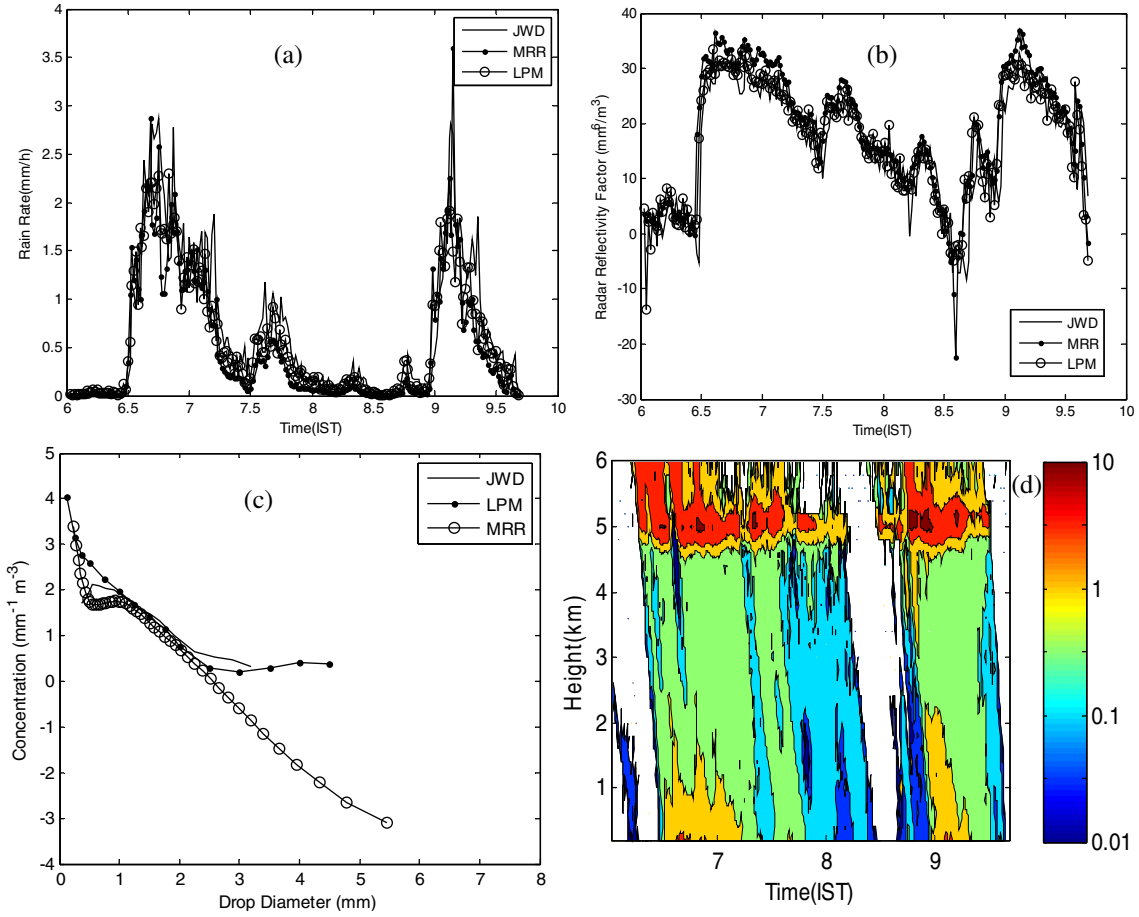

Fig. 3. Low rain rate event of 13 July 2013: (a) Ground rain rate, (b) Radar reflectivity (c) Ground DSDs' concentration in log10 scale for different drop diameters and (d) Height profile of rain rate in mm/h obtained from MRR.

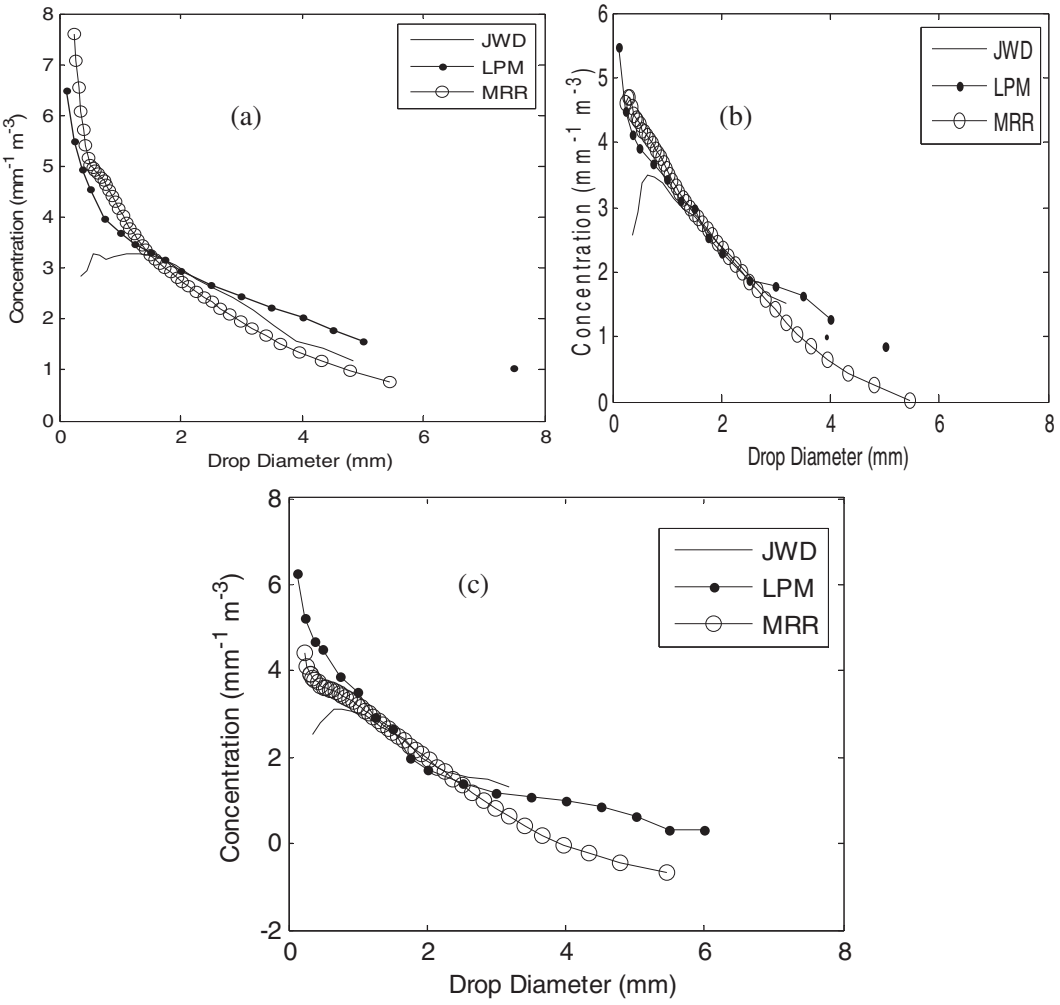

Fig. 4. Ground DSDs' concentration for different drop diameters: (a) Convective events, (b) Mixed events and (c) Stratiform events.

size measurements. The peak of the DSDs is just below 1 mm (Fig. 5(a–d)) in JWD, which shifts towards higher drop size (~2 mm) at high rain rates. Fig. 5(e) and (f) confirms that especially for very high rain rates, the ability of JWD decreases in sensing small drops. The ringing of the sensor diaphragm due to large raindrops impacts may be the reason of shadowing the information of the presence of small drops. This finding is also supported by Tokay et al. (2001) and Caracciolo et al. (2006). On the contrary, due to optical sensing, LPM is highly capable of detecting very small drops (<0.5). In each case, irrespective of rain rate intensity LPM measures very high concentration of small drops. Moreover LPM can detect very large drops >5.5 mm as shown in Fig. 5(d) and (f).

For low rain rates, below 2 mm/h, as shown in Fig. 5(a) and (b), the MRR observation overestimates both JWD and LPM data above 1 mm drop size range. MRR ground level is taken at a height range of 200 m but LPM and JWD disdrometer observations are taken near ground. In the case of very light rain rate, small to medium size DSDs contribute more and they are very vulnerable to weather parameters. The drop evolution mechanism via evaporation, break up and coalescence as well wind motion may be the cause of underestimation of DSD concentration in LPM and JWD compared to MRR. However for very small drops, LPM value is larger than both MRR and JWD. In this rain rate regime though MRR and LPM observe DSDs as large as 5 mm, JWD does not show any drop beyond 4 mm.

Fig. 5(c)–(d) shows the DSD concentration variation for medium rain rate range (<10 mm/h). A good matching of JWD, MRR and LPM is observed for 1–4 mm drop size range. However in this range of rain rate, LPM and MRR show a good agreement for large drop size values up to 6 mm drop size, but JWD shows drop sizes only up to 4 mm.

Similarly, the matching among the instruments is significant only in the range of 1.5 mm to 3 mm at rain events above 10 mm rain rate as the DSD peak shifts towards the high value. The MRR and LPM show similar values of drop concentration up to 5.5 mm, but the matching with JWD is poor at both ends. The matching with JWD and other two instruments is even worse in case of rain rate above 20 mm/h for large drop sizes (>3.5 mm) as shown in Fig. 5(f).

4.2.3. Rain rate comparison

The rain rate comparisons are shown in Fig. 6. Fig. 6(a) gives the scatter plots of rain rates measured by the pair of

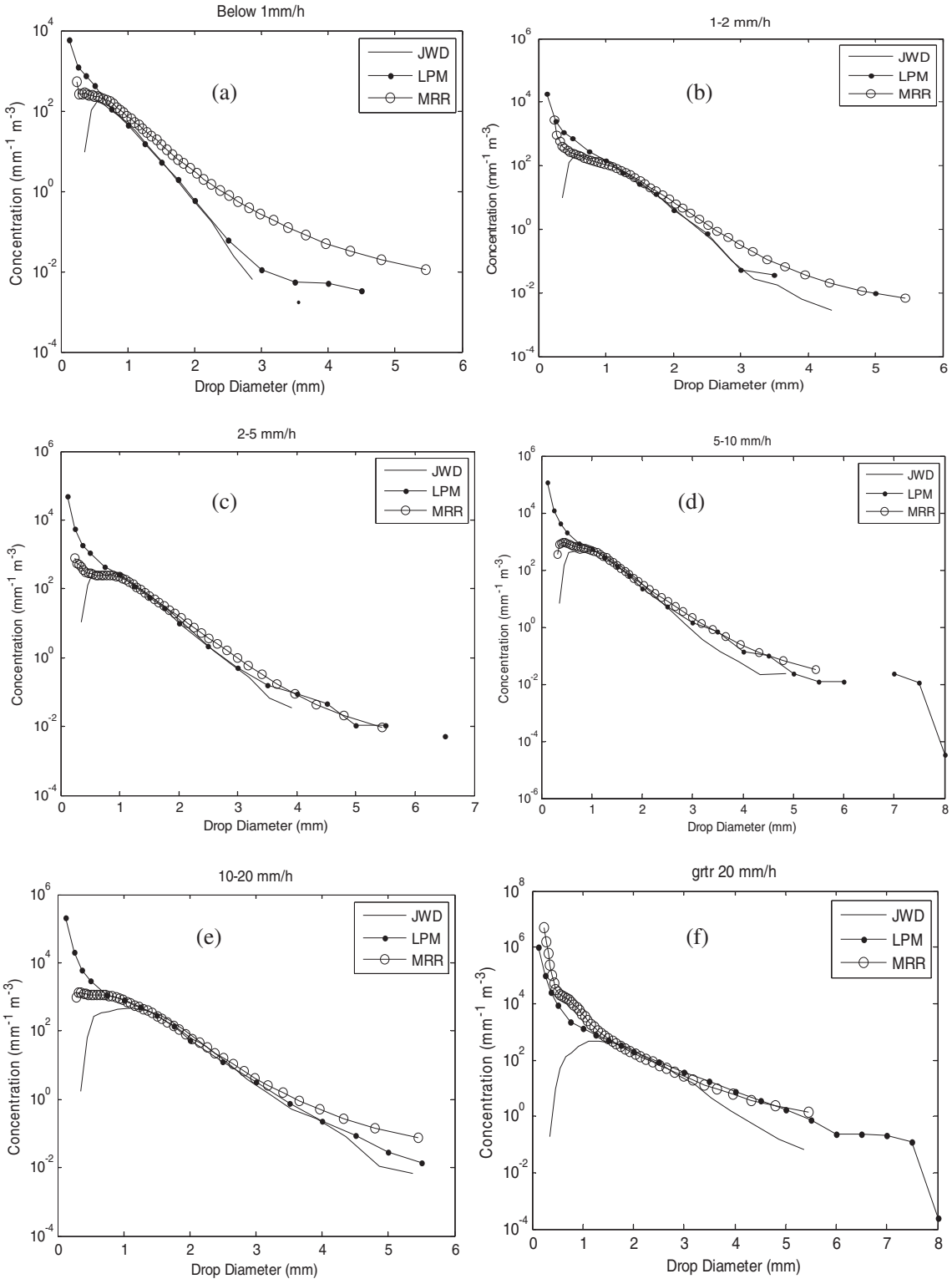

Fig. 5. DSD concentration vs. drop diameter for rain rates (a) Below 1 mm/h, (b) 1–2 mm/h, (c) 2–5 mm/h, (d) 5–10 mm/h, (e) 10–20 mm/h and (f) Greater than 20 mm/h.

instruments. The comparison shows better agreement between LPM and MRR rather than JWD and MRR or LPM and JWD. MRR and JWD recorded rain rates show a good agreement up to around 50 mm/h, beyond this rain rate range MRR tends to observe higher rain rates. However LPM observation matches well with MRR up to 80 mm/h rain rate range. LPM observes

higher rain rates beyond the range of 50 mm/h when compared with JWD.

From the performance indicators we can observe that for both rain rate measurements the R^2 values are more than 0.5 indicating high correlation among the measurements from the three instruments.

The MAE represents the average magnitude of the errors where individual differences are weighted equally whereas the RMSE gives a relatively high weight to large errors. The difference between RMSE and MAE thus indicate the variance of data points. From RMSE and MAE values of Fig. 6(a) we can observe that the variance of data points for rain rate data is maximum for LPM and JWD and minimum between JWD and MRR.

To better understand the inter-comparison among the instrumental measurements for rain rates, the probabilistic values of different quantiles are compared in Fig. 6(b). Quantiles refer to the fraction of data points below a given value and a

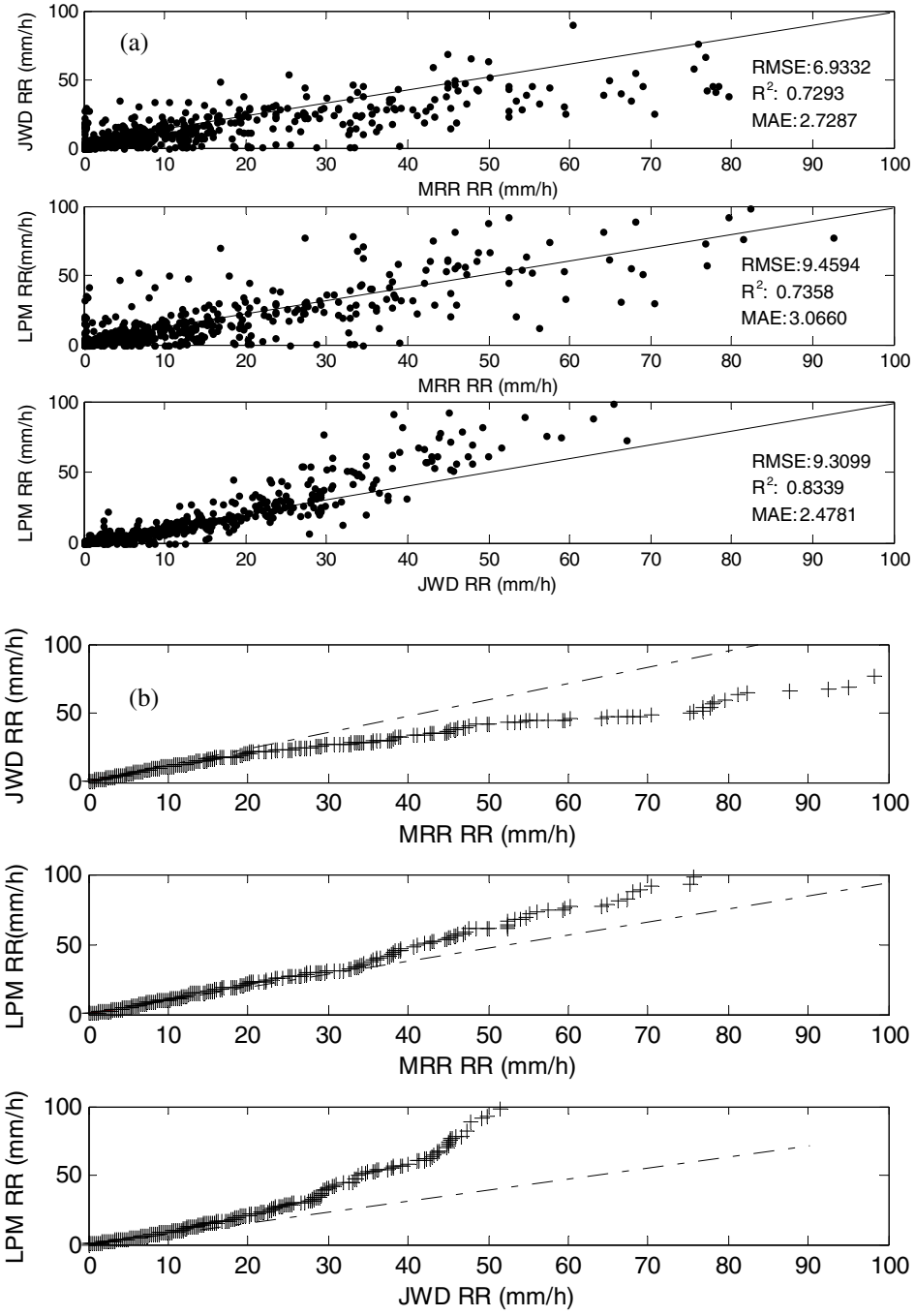

Fig. 6. (a) Scatter plot of rain rates obtained from different pairs of instruments, (b) Rain rate probability quantile plot from different pairs of instruments.

quantile–quantile plot can provide useful information as to what extent the distributions of the two data sets is similar. The probability distributions are estimated from the experimental observations of each instrument. The dotted line indicates the equal probability of two sets of observational data from the instruments which means that the experimental distributions

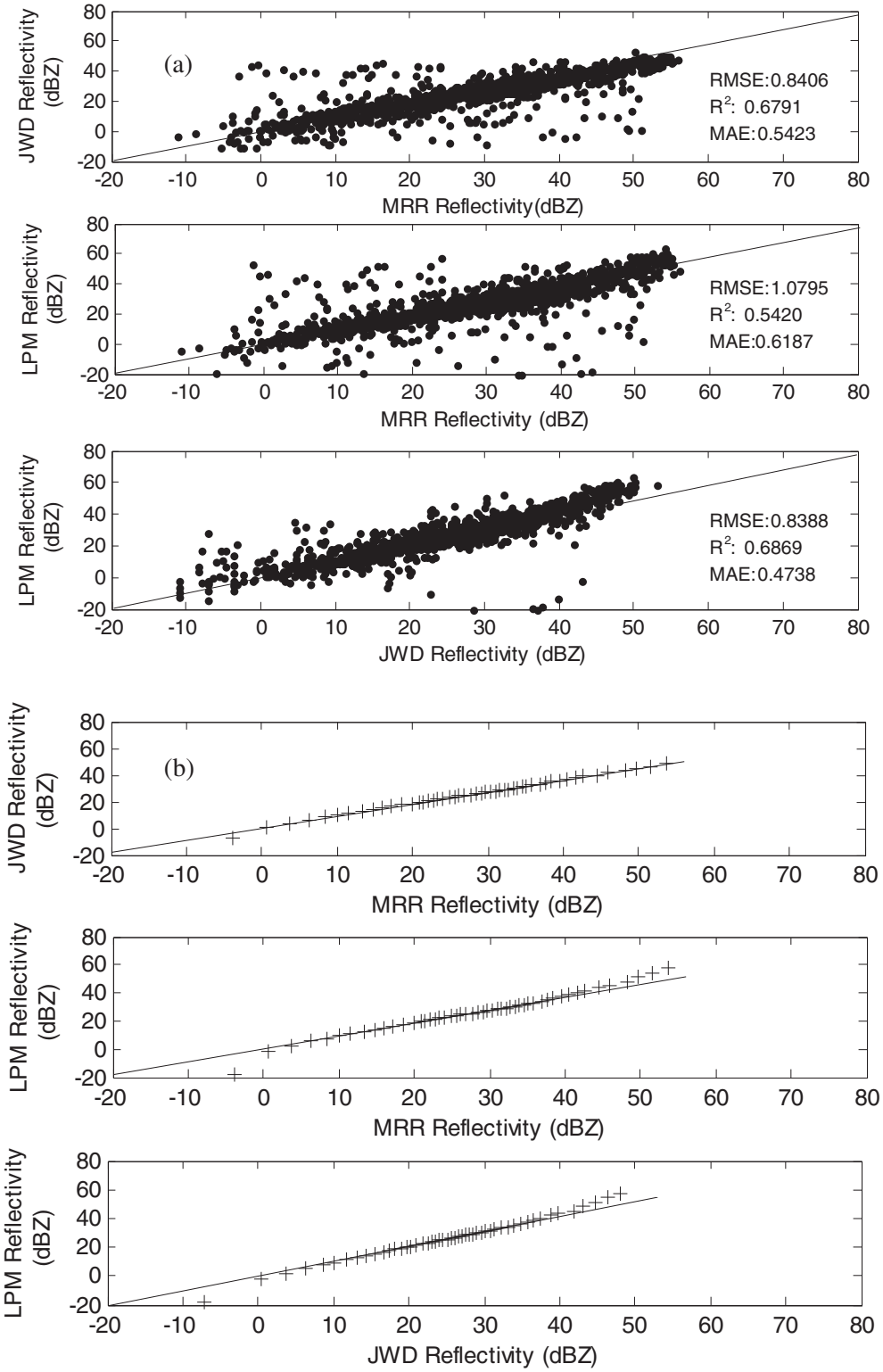

Fig. 7. (a) Scatter plot of radar reflectivity obtained from different pairs of instruments, (b) Probability quantile plot of radar reflectivity obtained from different pairs of instruments.

are of the same type. Up to 40 mm/h rain rates both MRR and JWD disdrometer show the same probability of detecting rain rates, whereas beyond this range MRR is more prone to detect high rain rate in comparison to JWD. LPM and MRR probability matches up to 60 mm/h and beyond this value LPM has the largest probability of showing higher rain rates compared to that measured by MRR. However JWD has less probability of measuring high rain rates compared to LPM beyond 30 mm/h.

4.2.4. Radar reflectivity factor comparison

A statistical comparison of radar reflectivity factor for all three instruments is shown in Fig. 7. One on one comparisons between the instruments show the best agreement in calculating Z between LPM and JWD. It is evident from Fig. 7(a) that the data scattered much less for LPM and JWD compared to the other two comparisons. The largest variability in *Z* is observed in the case of LPM and MRR measurements. However JWD and MRR matching is also quite good especially for higher Z values. As observed from the RMSE and MAE in Fig. 7(a) the variance in data points for radar reflectivity is maximum for LPM and MRR and minimum for JWD and MRR. Here also the $\boldsymbol{R}^2$ values are greater than 0.5, which shows high correlation among data points. Quantiles of probability for different pairs of instruments are presented in Fig. 7(b) for better depiction of the comparative performance. For very low values of *Z*, mutual agreement among the instruments is low. Probability of observing lower values of Z is higher for both MRR and JWD than LPM. However probability of observing Z beyond 40 dBZ is higher for LPM than JWD and MRR.

4.2.5. Z–R relation comparison

The inter-comparison of *Z–R* relationship is shown in Fig. (8) which is very much dependent on instruments as well as regression methods to determine the relationship (Campos and Zawadzki, 2000; Tokay et al., 2001). Campos and Zawadzki (2000) showed that the linear and non-linear regression methods give different results. In our case we have only taken linear regression, as our main objective is to differentiate between the instrumental capabilities. The *Z–R* relation is

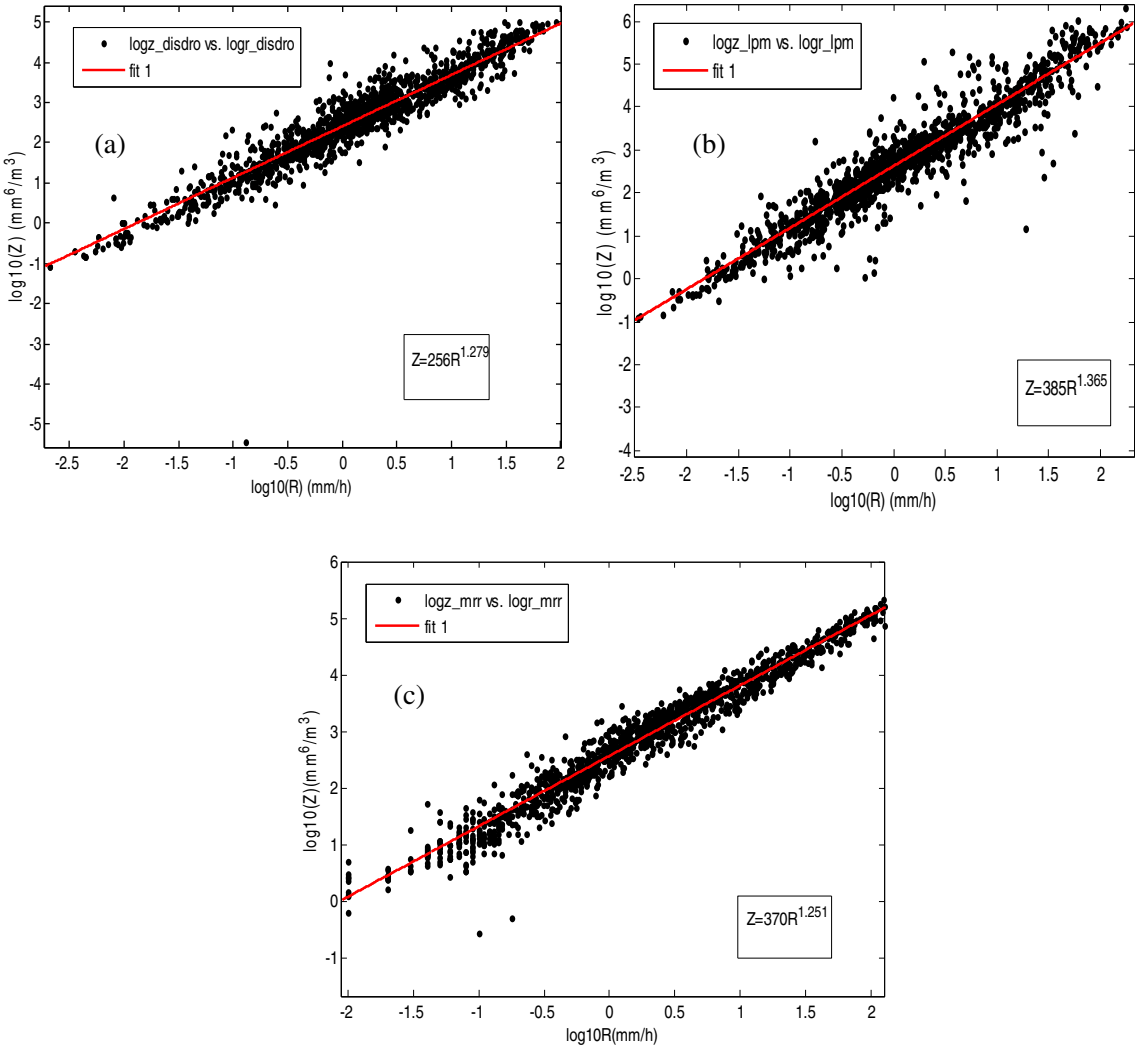

Fig. 8. Z–R plot for (a) JWD, (b) MRR, (c) LPM.

Table 5
The values of '*a*', '*b*' and chi-square test.

Instrument	'*a*'	'*b*'	χ^2 error
JWD	256	1.279	344.6487
LPM	385	1.365	702.9587
MRR	370	1.251	645.5096

derived from the full data set without stratiform and convective classification for different instruments separately.

In implementing linear regression, the relation, $Z = aR^b$, is expresses as follows:

$$log_{10}(Z) = log_{10}(a) + blog_{10}R. \quad (4)$$

The values of '*a*' and '*b*' are calculated from the data using linear regression. The parameters '*a*' and '*b*' and associated χ^2 value of the fitting is shown in Table 5. The χ^2 error statistics is defined as the sum of the square of difference between Z calculated from experimental values and Z calculated from the linear regression.

It can be observed from χ^2 values in Table 5 that LPM has highest dispersion in data points than the fitted curve, whereas the spread associated with JWD is the least. Although it is expected to be less dispersed in case of MRR due to larger sampling volume (Campos and Zawadzki, 2000), however our findings show larger χ^2 value for MRR in comparison with JWD. These results can be explained in accordance to the findings of Zawadzki (1984) and Chandrasekar and Bringi (1987) in which it is shown that a larger error is associated with larger sampling volumes compared to the instruments with smaller sampling volume which come from the decreasing statistical correlation among data points in larger sampling volume. The '*a*' value is highest for LPM and lowest for JWD and '*b*' is largest for LPM and lowest for MRR.

5. Conclusions

DSD is one of the most important parameters to study the microstructure of rain. On the other hand, *Z–R* relation is required for radar remote sensing which can be derived from DSD measurements. In this paper an attempt has been made to evaluate performance of JWD, MRR and LPM. This will help to analyze different drop measuring techniques and assess their advantages and limitations in different rain rate regimes.

All these instruments are found to measure similar rain rates up to ~30 mm/h. The estimated radar reflectivity factor is in good agreement among all instruments only in the range of 10–40 dB. However, the Z–R relation estimated from different instrument showed significant variations. Similar drop concentrations are found to be measured by all these three instruments between 1 and 3 mm but this agreement does not hold for very small or very large drops.

JWD, due to its electro-mechanical working principle, is less sensitive in detecting very small drops (<0.5 mm) and does not measure drops beyond the range of 5.5 mm. It is a widely used instrument and measures rain DSDs quite efficiently, especially the medium drop sizes. Thus the instrument is reliable in case of measuring rain rate and radar reflectivity factor for rain events that are not too low (<0.1 mm/h) or too high (>20 mm/h).

The LPM works on the basis of optical principle and is very sensitive in measuring low intensity rain events. It can measure smallest drops (<0.5 mm) very efficiently. As it erroneously senses simultaneously falling drops as one large drop, it can give unreasonable high value of drop size for high rain rate events.

MRR is a useful instrument, using radio technique, for getting height profile of rain integral parameters. However for ground measurements, especially low rain rate events, it overestimates the drop concentration. For medium to high rain rates, it gives reliable results for drop sizes up to 3 mm.

We observed that it is not practically possible to measure accurately all sizes of drops with every instrument due to its operating principle. However, the present study identifies ranges in which reliable measurements are possible for different instruments.

Other than the working principles mentioned, high wind velocity will affect the DSDs' measurements, which may give some error in results, especially in high convective phenomena. The effect of wind in DSD measurements will be most pronounced in the case of LPM measurements as the horizontal component of wind will affect the number of drops in the small slit of the instrument. However the effect of vertical wind motion will be reflected in the measurements of all the instruments mentioned here. Different sampling volumes of the instruments can also lead to mismatch in the measured rain parameters by different instruments. LPM has the smallest sampling volume whereas MRR has the largest sampling volume. Further MRR measures the raindrops at some height above the ground, so height evolution of the raindrops can also alter the DSDs. The error reported here is a combination of both sampling error as well as instrumental working principle. It may be noted that, with the present experimental setup, it is not possible to quantify the individual components of error in the measurements of instruments working with different principles. In the present study it is intended to indicate the ranges of rainfall parameters in which the instruments can work with reasonable reliability.

Acknowledgments

Financial support provided under, (1) TEQIP Phase II (TEQIP-II/ACA/2013/70) and (2) ISRO (E 33013/3/2009-V) sponsored "Space Science Promotion Scheme", are thankfully acknowledged.

References

Campos, E., Zawadzki, I., 2000. Instrumental uncertainties in Z–R relations. J. Appl. Meteorol. 39, 1088–1102. http://dx.doi.org/10.1175/1520-450(2000)039<1088:IUIZRR>2.0.CO;2.

Caracciolo, C., Prodi, F., Uijlenhoet, R., 2006. Comparison between Pludix and impact/optical disdrometers during rainfall measurement campaigns. Atmos. Res. 82 (1–2), 137–163.

Chandrasekar, V., Bringi, V.N., 1987. Simulation of radar reflectivity and surface measurements of rainfall. J. Atmos. Ocean. Technol. 4, 464–478.

Chen, B., Hu, W., Pu, J., 2011. Characteristics of the raindrop size distribution for freezing precipitation observed in southern China. J. Geophys. Res. 116, D06201. http://dx.doi.org/10.1029/2010JD015305.

Das, S., Maitra, A., Shukla, A.K., 2010. Rain attenuation modeling in the 10–100 GHz frequency using drop size distributions for different climatic zones in tropical India. Prog. Electromagn. Res. B 25, 211–224.

Fabry, F., Zawadzki, I., 1995. Long-term radar observations of the melting layer of precipitation and their interpretation. J. Atmos. Sci. 52, 838–851.

Frasson, R.P.M., Cunha, L.K., Krajewski, W.F., 2011. Assessment of the Thies optical disdrometer performance. Atmos. Res. 101, 237–255.
Gunn, R., Kinzer, Gilbert D., 1949. The terminal velocity of fall for water droplets in stagnant air. J. Meteorol. 6, 243–248.
Islam, T., Rico-Ramirez, M.A., Thurai, M., Han, D., 2012. Characteristics of raindrop spectra as normalized gamma distribution from a Joss–Waldvogel disdrometer. Atmos. Res. 108, 57–73.
Jaffrain, J., Berne, A., 2011. Experimental quantification of the sampling uncertainty associated with measurements from Parsivel disdrometers. J. Hydrometeorol. 12, 352–370.
Kain, J.S., Goss, S.M., Baldwin, M.E., 2000. The melting effect as a factor in precipitation-type forecasting. Weather Forecast. 15, 700–714.
Lanzinger, E., Theel, M., Windolph, H., 2006. Rainfall amount and intensity measured by the THIES laser precipitation monitor. TECO-2006, Geneva, Switzerland. 2006 — wmo.int.
Peters, G., Fischer, B., Andersson, T., 2002. Rain observations with a vertically looking Micro Rain Radar (MRR). Boreal Environ. Res. 7, 353–362.
Peters, G., Fischer, B., Münster, H., Clemen, M., Wagner, A., 2005. Profiles of raindrop size distributions as retrieved by microrain radars. J. Appl. Meteorol. 44, 1930–1949.
Rao, T.N., Radhakrishna, B., Nakamura, K., Rao, N.P., 2009. Differences in raindrop size distribution from southwest monsoon to northeast monsoon at Gadanki. Q. J. R. Meteorol. Soc. 135, 1630–1637.
Reddy, K.K., Kozu, T., 2003. Measurements of raindrop size distribution over Gadanki during south-east and north-east monsoon. Indian J. Radio Space Phys. 32, 286–295.
Sarkar, T., Das, S., Maitra, A., 2014. Effects of melting layer on Ku-band signal depolarization. J. Atmos. Sol. Terr. Phys. 144, 95–110.
Sheppard, B.E., Joe, P.I., 1994. Comparison of raindrop size distribution measurements by a Joss–Waldvogel disdrometer, a PMS 2DG spectrometer and a POSS Doppler radar. J. Atmos. Ocean. Technol. 11, 874–887.
Steiner, M., Houze, R.A., Yuter, S.E., 1995. Climatological characterization of three dimensional storm structure from operational radar and rain gauge data. J. Appl. Meteorol. 34, 1978–2007.
Sun, J., Zhao, S., 2010. The impacts of multi scale weather systems on freezing rain and snow storms over the southern China. Weather Forecast. 25, 388–407. http://dx.doi.org/10.1175/2009WAF2222253.1.
Thurai, M., Bringi, V.N., Carey, L.D., Gatlin, P., Schultz, E., Petersen, W.A., 2012. Estimating the accuracy of polarimetric radar-based retrievals of drop-size distribution parameters and rain rate: an application of error variance separation using radar-derived spatial correlations. J. Hydrometeorol. 13, 1066–1079. http://dx.doi.org/10.1175/JHM-D-11-070.1.
Thurai, M., Williams, C.R., Bringi, V.N., 2014. Examining the correlations between drop size distribution parameters using data from two side-by-side 2D-video disdrometers. Atmos. Res. 144, 95–110.
Tokay, A., Short, D., 1996. Evidence from tropical raindrop spectra of the origin of rain from stratiform versus convective. J. Appl. Meteorol. 35, 355–371.
Tokay, A., Short, D.A., Williams, C.R., Ecklund, W.L., Gage, K.S., 1998. Tropical rainfall associated with convective and stratiform clouds: intercomparison of disdrometer and profiler measurements. J. Appl. Meteorol. 38, 302–320.
Tokay, A., Kruger, A., Krajewski, W.F., 2001. Comparison of drop size distribution measurements by impact and optical disdrometers. J. Appl. Meteorol. 40, 2083–2097.
Tokay, A., Petersen, W.A., Gatlin, P., Wingo, 2013. Comparison of raindrop size distribution measurements by collocated disdrometers. J. Atmos. Ocean. Technol. 30, 1672–1690. http://dx.doi.org/10.1175/JTECH-D-12-00163.1.
Ulbrich, C.W., Atlas, D., 2007. Microphysics of raindrop size spectra: tropical continental and maritime storms. J. Clim. Appl. Meteorol. 46, 1777–1791. http://dx.doi.org/10.1175/2007JAMC1649.1.
Zawadzki, I., 1984. Factors affecting the precision of radar measurements of rain. Preprints. 22d Conf. on Radar Meteorology. Amer. Meteor. Soc, Zurich, Switzerland, pp. 251–256.
Zhou, W., Chan, J.C.L., Chen, W., Ling, J., Pinto, J.G., Shao, Y., 2009. Synoptic scale controls of persistent low temperature and icy weather over Southern China in January 2008. Mon. Weather Rev. 137, 3978–3991. http://dx.doi.org/10.1175/2009MWR2952.1.